

Heterogeneous coverage method with multiple unmanned aerial vehicle assisted sink nodes^①

Jin Shan(金 杉)^{②* **}, Jin Zhigang^{*}

(^{*} Electrical, Automation and Information Engineering College, Tianjin University, Tianjin 300072, P. R. China)

(^{**} Fire and Rescue Department, Bureau of Emergency Management of Tianjin, Tianjin 300090, P. R. China)

Abstract

A heterogeneous coverage method with multiple unmanned aerial vehicle assisted sink nodes (MUAUVs) for multi-objective optimization problem (MOP) is proposed, which is based on quantum wolf pack evolution algorithm (QWPEA) and power law entropy (PLE) theory. The method is composed of preset move and autonomous coordination stages for satisfying non-repeated coverage, connectedness, and energy balance of sink layer critical requirements, which is actualized to cover sensors layer in large-scale outside wireless sensor networks (WSNs). Simulation results show that the performance of the proposed technique is better than the existing related coverage technique.

Key words: wireless sensor network (WSN), coverage, multi-unmanned aerial vehicle (MUAUV), heterogeneous, sink node, quantum wolf pack evolution algorithm (QWPEA), power law entropy (PLE)

0 Introduction

Multi-unmanned aerial vehicle assisted wireless sensor networks (MUAUV-WSNs) are composed of MUAUVs and WSNs, which are widely applied in civil and military affairs^[1]. In recent years, MUAUV-WSNs have broad prospects in large-scale WSNs coverage. Nevertheless, the problems including low detected frequency, small shoot range, and unbalanced energy consumption become more serious than before.

Recently, there are 2 modalities of MUAUV-WSNs application, including research and communication relay. MUAUV-WSNs are utilized for relaying between fixed or mobile facilities in Refs[2] and [3]. And in Ref. [4], they are used in film videos and data transmission with frontier-based exploration algorithm for resolving the communication and energy consumption problems. In summary, the former application modalities are mature, operable and stable. However, their applications in media information detection and communication relay limit dominance of MUAUV-WSNs' realizing multi-objectives. Also, these methods are exposed with meteorological interference.

In this paper, MUAUV-WSNs are utilized to cover plenty of sensors on the earth for sink, transmission, and

relaying use. And the QWE-PLE algorithm is proposed. Specifically, the quantum wolf pack evolution algorithm (QWPEA) and power law entropy (PLE) theory are utilized to be designed into preset move and autonomous coordination stages for the sub-objectives including non-repeated coverage, connectedness, and balanced energy consumption. Simulation results show that the performance of the proposed method is better than that of the existing coverage technique.

1 System model

UAVs' models with GPS systems are identical completely. Also, their initial battery reserves are equal. And sensors are deployed on the detected area heterogeneously. Flight height h_f is a preset value, and surface elevation is h_m . Therefore, $h_f \gg h_m$ and $h_m \approx 0$ are existence for flight safety. Then a circular coverage projection is shaped from each multi-unmanned aerial vehicle assisted sink node (MUAUVS).

The improved duality perceptive model^[5] is utilized to simulate the WSNs' communications with 2-layer topology structure. Specifically, the sink nodes set $C_{\text{sink}} = \{c_1, c_2, \dots, c_N\}$ on the deployment area A_{net} . And the model from any of sink node is $c_i = \{x_i, y_i, z_i, r^w, r^z\}$. Its coordinate is (x_i, y_i, z_i) . Then

① Supported by the National Natural Science Foundation of China (No. 61571318), Key Research and Development Project of Hainan (No. ZDYF2018006), Independent Innovation Fund of Tianjin University and Doctoral Fund Funded Projects.

② To whom correspondence should be addressed. E-mail: shanye2006@163.com

Received on Dec. 9, 2018

the different frequencies communication models including Wi-Fi and ZigBee are installed in each sink node. The Wi-Fi link is utilized for sink layer's communication, whose range is r^w . Similarly, the ZigBee link, whose radius is r^z , is for transmission between sink and sensor layers. And there exists $r_i^w \geq r_i^z$. In addition, r_i^z is the surface projection and there is:

$$r_i^z = \text{sqr}[(r_i^w)^2 - (h_f - h_m)^2] \quad (1)$$

The communication area A_s of each MUAWS for connection in sink layer is:

$$A_s = \sum_{i=1}^N \pi (r_i^w)^2 \quad (2)$$

In preset move stage, the location information is detected and transmitted, whose data packets are too small to count. Nevertheless, the MUAWS i obtains L' bits in autonomous coordination stage of any period T_i . For instance, it sends 1 bit data with energy consumption e_1 . Also, it receives 1 bit with energy cost e_2 . Likewise, it transmits data packets to U neighbor sink nodes with energy consumption E_{receive} for receiving. Therefore, MUAWS i is actualized with the packets transmission with energy cost $E_{\text{all}, i}$. There is:

$$E_{\text{all}, i} = \sum_{i=1}^U L'_i \cdot e_1 + \sum_{i=1}^U L'_i \cdot e_2 \quad (3)$$

Furthermore, the flight energy consumption $E_{\text{fly}, i}$ of MUAWS i is just related to flight duration $t_{\text{fly}, i}$. If flight energy cost parameter is ν , the residual energy $E_{\text{ex}, i}$ is:

$$E_{\text{ex}, i} = E_{\text{org}} - T_i E_{\text{all}, i} - E_{\text{fly}, i} \quad (4)$$

where $E_{\text{fly}, i} = \nu t_{\text{fly}, i}$. Fig. 1 shows MUAWS' coverage.

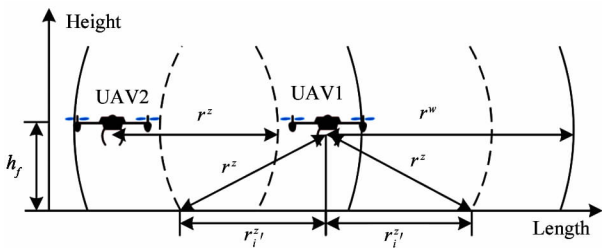


Fig. 1 MUAWS' coverage states

2 Proposed method

In this work, the multi-objective optimization problem (MOP)^[6] is composed of 3 sub-problems including coverage, connection, and balanced energy consumption. Then the MUAWS coverage process is divided into preset move and autonomous coordination stages. Firstly, all MUAWSs fly to the preset target. Secondly, autonomous coordination stage runs in circles, until the system can meet the

need of each sub-objective or achieve maximum number of iterations.

Definition 1 Effective coverage ratio R_{area} (C_{sink}). The ratio is between non-overlapping effective coverage size $A_{\text{area}}(C_{\text{sink}})$ and communication area A_s . And g of it is the number of coverage layers, $A_{\text{cov}}(x_i, y_i, z_i, C_{\text{sink}})$ is the coverage size of MUAWS i , and $A_{\text{ex}}(c_i, g)$ is the summation of redundant coverage sizes, which are intersected with c_i .

$$R_{\text{area}}(C_{\text{sink}}) = A_{\text{area}}(C_{\text{sink}}) / A_s$$

$$= \sum_{i=1}^N \left\{ \left[A_{\text{cov}}(x_i, y_i, z_i, C_{\text{sink}}) - \sum_{g=1}^{\lambda_i} \left(\frac{g-1}{g} A_{\text{ex}}(c_i, g) \right) \right] / \pi (r_i^w)^2 \right\};$$

$$g, \lambda_i \in N^+, g < \lambda_i \quad (5)$$

Definition 2 Cross-layer connected ratio R_{s-s} . The ratio is between the number of connected MUAWSs and sensors. If R_{s-s} is less, sensors are more central. It means that the deployment of sink layer is more dynamic.

$$R_{s-s} = \sum_{i=1}^N [P(\sum_{j=1}^{N-1} P(d(c_i, c_j) \leq r^w) > 0)] / N_s \quad (6)$$

where, $d(c_i, c_j)$ is the distance between the connected MUAWSs c_i and c_j . $P(d(c_i, c_j) \leq r^w) = 1$ means the former 2 MUAWSs are connected. Therefore, $P(\sum_{j=1}^{N-1} P(d(c_i, c_j) \leq r^w) > 0) > 0$ means that MUAWS c_i is connected with sink layer.

Definition 3 Communication energy cost ratio R_{Ecc} . The ratio is between MUAWSs' communication energy consumption E_{cc} and $E_{\text{all-C}}$, which stands for that of MUAWS-WSNs. And node communication parameter u is utilized to adjust the transmission state of MUAWS i .

$$R_{\text{Ecc}} = E_{\text{cc}} / E_{\text{all-C}}$$

$$= u \times \left(\sum_{i=1}^N (r_i^w)^2 + \sum_{k=1}^{N+M} (r_k^z)^2 \right) / E_{\text{all-C}} \quad (7)$$

In summary, $R_{\text{area}}(C_{\text{sink}})$, R_{s-s} , and R_{Ecc} are sub-objectives for optimization at the same time completely. And the balance among them is actualized with weighted method.

$$\min f(x) = \begin{cases} f_1(x_1) = 1 - R_{\text{area}} \\ f_2(x_2) = R_{s-s} \\ f_3(x_3) = 1 - R_{\text{Ecc}} \end{cases} \quad (8)$$

$$f_{\text{obj}}(x) = \sum_{i=1}^K w_i n_i f_i(x_i), \quad \sum_{i=1}^K w_i = 1 \quad (9)$$

where $f_{\text{obj}}(x)$ is general objective function, K is the number of sub-objectives, n_i is normalization constant, and w_i is weight. Here $w_1 + w_2 + w_3 = 1$ and $K = 3$. Therefore, the optimum solution is obtained from the minimum of $f_{\text{obj}}(x) \in (0, 1)$.

At the preset move stage, the target positions are pre-optimized for multi-objective by quantum wolf pack evolutionary algorithm (QWPEA). Then MUAVs fly straight forward there.

Each quantum state of artificial wolf coding is set as $|\Psi\rangle$:

$$|\Psi\rangle = \alpha|0\rangle + \beta|1\rangle \quad (10)$$

where α and β stand for probability amplitudes of quantum corresponding state. $|\alpha|^2$ stands for probability of $|0\rangle$, and $|\beta|^2$ is that of $|\Psi\rangle$.

N MUAVSs and M sensor nodes are coded as coverage matrix C and cascade matrix S . And $c_{m,n}, s_{m,n} \in \{0, 1\}$ exists. Furthermore, while $c_{m,n} = 1$ in matrix C , $s_{m,n}$ in matrix S is coded from lines to rows. There are:

$$C = \begin{bmatrix} c_{1,1} & c_{1,2} & \cdots & c_{1,N} \\ c_{2,1} & c_{2,2} & \cdots & c_{2,N} \\ \vdots & \vdots & & \vdots \\ c_{M,1} & c_{M,2} & \cdots & c_{M,N} \end{bmatrix}$$

$$S = \begin{bmatrix} s_{1,1} & s_{1,2} & \cdots & s_{1,N} \\ s_{2,1} & s_{2,2} & \cdots & s_{2,N} \\ \vdots & \vdots & & \vdots \\ s_{M,1} & s_{M,2} & \cdots & s_{M,N} \end{bmatrix} \quad (11)$$

The initial probability amplitudes of quantum corresponding states emerge from Logistic chaotic map, which is $\mu_{\text{chaos}} = 4$.

$$x_{k+1} = \mu_{\text{chaos}} x_k (1 - x_k) \quad k \in N \quad (12)$$

The leader wolf is in iteration directly, which is the nearest to the initial optimal general objective function. Then the quantum state of each wolf needs to be measured.

$$z_l = \begin{cases} 0 & \text{random}[0, 1] > |\alpha_l|^2 \\ 1 & \text{random}[0, 1] \leq |\alpha_l|^2 \end{cases} \quad (13)$$

where $Z = (z_1, z_2, \dots, z_L)$ is the binary solution after measuring states. Then they are transformed to binary series codes to compose the corresponding objective coverage projects. If the new solution is better than the current optimum solution Z_{best} , all of that will be refreshed to compose a set Z^{candi} , which contains the candidate leader wolves (CLW).

Subsequently, the evolution is actualized. Fig.2 shows that the method is genetic evolution based on cross quantum in sliding mode theory. And it expands the directed solution space. Then the elements in solutions set Z^{candi} are sorted from optimum to the suboptimum to cross with leader wolf's chromosomes as the sliding mode method. In addition, cross parameter w_i^c defers to Gaussian distribution. Moreover, the single-point crossover starts from the low quantum at the right end of chromosomes.

$$f_{\text{gauss}}(e_i^c) = \frac{1}{\sqrt{2\pi}\sigma} e^{-(e_i^c - \mu)^2 / 2\sigma^2} \quad (14)$$

where $Z_i^{\text{candi}} = (z_{i,1}^{\text{candi}}, z_{i,2}^{\text{candi}}, \dots, z_{i,j}^{\text{candi}}, \dots, z_{i,L}^{\text{candi}})$, $j \in L$ shows all the quantum j of CLW i is sorted. I is the number of CLW, and j_i^{slide} is the quantum meaning finished sliding-cross mode.

$$w_i^c = \int_{\frac{i-1}{I}\sigma}^{\frac{i+1}{I}\sigma} f_{\text{gauss}}(e_i^c) de_i^c \quad \sum_{i=1}^I w_i^c = 1 \quad (15)$$

$$j_i^{\text{slide}} = \begin{cases} L & w_i^c \in [0, I^{-1}] \\ \lfloor L \times (1 - w_i^c) \rfloor & w_i^c \in (I^{-1}, (I-2) \cdot I^{-1}] \\ 2 & w_i^c \in ((I-2) \cdot I^{-1}, 1] \end{cases} \quad (16)$$

Therefore, while CLW is the optimum solution, w_i^c reaches minimum value, and the new solution space is near the existing solutions. In contrast, if w_i^c is higher, the new solution space will have more changes.

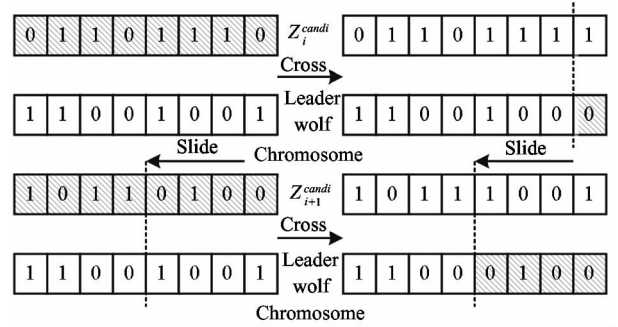


Fig. 2 Sliding-cross method

Then update of the quantum rotation gate and control to non quantum gate are utilized on each quantum of newest iterate wolves with the current optimum solution.

$$\begin{bmatrix} \alpha_l^{\text{new}} \\ \beta_l^{\text{new}} \end{bmatrix} = \begin{bmatrix} \cos\theta & -\sin\theta \\ \sin\theta & \cos\theta \end{bmatrix} \begin{bmatrix} \alpha_l \\ \beta_l \end{bmatrix} \quad (17)$$

$$\begin{bmatrix} \beta_l \\ \alpha_l \end{bmatrix} = \begin{bmatrix} 0 & 1 \\ 1 & 0 \end{bmatrix} \begin{bmatrix} \alpha_l \\ \beta_l \end{bmatrix} \quad (18)$$

where α_l^{new} and β_l^{new} stand for probability amplitudes of quantum corresponding state after refreshing. Similarly, α_l and β_l are that of before refreshing.

In the autonomous coordination stage, the locations of sensors are analyzed. And n_{cl} sensor dense centers O_k are clustered with the SUBFCM algorithm in Ref. [7]. Then the connected MUAVSs move forward or away from these centers with the power law entropy method from the quadratic entropy theory^[8]. Moreover, PLE has great effect on multi-objective.

Definition 4 Average coverage distance \bar{L}_i^{sen} . The distance is between MUAVS and any of covered sensors j which stands for the sensors clustering states in the coverage area of MUAVS. And node communi-

cation parameter u is utilized to adjust the transmission state of MUAVS i . There is $\bar{L}_i^{\text{sen}} = (\text{sqr} \sum_{k=1}^K [(x_{\text{sen},k} - x_i)^2 + (y_{\text{sen},k} - y_i)^2 + (z_{\text{sen},k} - z_i)^2])/K$, where K is the number of sensors, covered by MUAVS. \bar{L}_i^{sen} and K decide the coverage quality of $A_{\text{cov}}(x_i, y_i, z_i, C_{\text{sink}})$.

Definition 5 Average connected distance \bar{L}_i^{sin} . It shows the square errors of Euclidean distance between directly connected MUAVSs. There is $\bar{L}_i^{\text{sin}} = (\text{sqr} \sum_{j=1}^J [(x_j - x_i)^2 + (y_j - y_i)^2])/J$, where J is the number of directly connected MUAVSs. \bar{L}_i^{sin} and J decide the connected quality in sink layer.

Similarly, while any of the flight duration $t_{\text{fly},i}$ is equal, and all the flight energy consumptions $E_{\text{fly},i}$ of MUAVSs are equal. Therefore, the transmission energy cost $E_{\text{all},i}$ and the number of iteration periods T_i in autonomous coordination stage decide the redundant energy $E_{\text{ex},i}$.

Quadratic entropy $S_{\text{sq},i}(t)$ is decided according to the probability distribution of variable t' . And the approximate valuation from entropy of information is obtained with it. At the autonomous coordination stage, the power law entropy S_{pl} based on quadratic entropy $S_{\text{sq},i}(t)$ is proposed to optimize all the sub-objectives.

Definition 6 Power law entropy (PLE) S_{pl} . It describes the MUAVS's dynamic state including transmission probability, connection level, and redundant energy.

$$S_{pl,i}(t) = \frac{S_{\text{sq},i}(t) K \bar{L}_i^{\text{sen}} T_i E_{\text{all},i}}{\bar{J} \bar{L}_i^{\text{sin}}} \quad (19)$$

where t is interval sampling time, and right side of equation is transformed as it. And the average PLE S_{pl,a,G_k} of n MUAVSs are selected from any of sensor dense area $G_k(O_k, R_k)$. The R_k is the area's radius, and $l_{G_k,j}$ is the j th equal spaced concentric circles in the area G_k . There is $l_{G_k,j} \in [0, R_k]$.

$$S_{pl,a,G_k}(l_{G_k,j}, t) = \frac{1}{n} \sum_{i=1}^n S_{pl,i}(l_{G_k,j}, t) \quad (20)$$

There is the PLE distribution $S_{pld,G_k}(t)$ in area G_k .

$$\begin{cases} S_{pld,G_k}(t) = \int_0^\infty \frac{S_{pl,a,G_k}(l_{G_k,j}, t)}{S_{pl-\max}(t)} dj \\ S_{pl-\max}(t) = \max\{S_{pl,i}(t)\} \\ i = 1, 2, \dots, n; \end{cases} \quad (21)$$

According to entropy theory, PLE is transformed towards entropy increase naturally. However, the PLE incremental quantity ΔS_{pl} is adjusted in period T_j of autonomous coordination stage. And the MUAVSs move

towards or away from the center O_k in the area G_k . Meanwhile, the PLE distribution S_{pld} is as reference coordinate, and $step_{abs}(l_{G_k,j}, T_j)$ is moving step. There is:

$$\begin{aligned} \Delta S_{pld,i} &= S_{pl,i}(l_{G_k,j}, t) - S_{pld,G_k}(t) \quad (22) \\ \begin{cases} step_{abs}(l_{G_k,j}, T_i) = 10(\alpha J / K T_i l_{G_k,j})^{1/2}, & \Delta S_{pld,i} < 0 \\ step_{abs}(l_{G_k,j}, T_i) = 0, & \Delta S_{pld,i} = 0 \\ step_{abs}(l_{G_k,j}, T_i) = -10(\alpha J / K T_i l_{G_k,j})^{1/2}, & \Delta S_{pld,i} > 0 \end{cases} \quad (23) \end{aligned}$$

where α is coordination parameter, and the positive direction is toward the center O_k .

3 Simulations

For the simulations, the detection area is set to 1 km^2 . The number of UAVs with single sink node is 16. And the 100 sensors are deployed as random locations. The related length parameters are $r_i^w = 220 \text{ m}$, $r_i^{z'} = 180 \text{ m}$, and $R_k = 200 \text{ m}$. Moreover, sending or receiving 1 bit energy consumption is $50 \times 10^{-8} \text{ J/bits}$. In the proposed algorithm, the sub-objective normalization constant $n_1 = 0.4$, $n_2 = 0.3$, $n_3 = 0.3$, and the coordination parameter $\alpha = 50$. In addition, the UAV's flight height h_f is 50 m, the surface elevation h_m is 0. And the battery's storage on each one is 4480 mA. The compared algorithms include virtual potential field (VPF)^[9], virtual force algorithm (VFA)^[10], and non-dominated sorting genetic algorithm-II (NSGA-II)^[11].

Fig. 3 shows that the sink layer effective coverage ratio is 89.6%, and the cross-layer connected ratio is 100% under stable state. At the preset move stage, each UAV flies straight forward to the target. Then 6 MUAVSs carry out optimization for 2 sensor dense areas in the autonomous coordination stage. In these areas, the higher PLE MUAVSs fly away from their related sensor dense centers, the lower flies towards the centers for the balanced energy consumption^[12-14].

In Fig. 4, the algorithms show that the residual energy mean variance ratios expand with the increasing iteration frequency. Nevertheless, its difference with QWE-PLE algorithm is less than the other's as entropy increases. The reason is that the autonomous coordination stage of the proposed method is based on the former global optimization. In contrast, the compared algorithms are merely devoted to the largest area than before. Therefore, the energy holes are easy to appear at sensor dense areas, where the consumption of sink nodes is faster than the else significantly. In experi-

ment, the result shows that the residual energy mean variance ratio with QWE-PLE method is 7.6%, while the iteration number is 50. And the ratio is 39.2% lower than that with the compared methods at least.

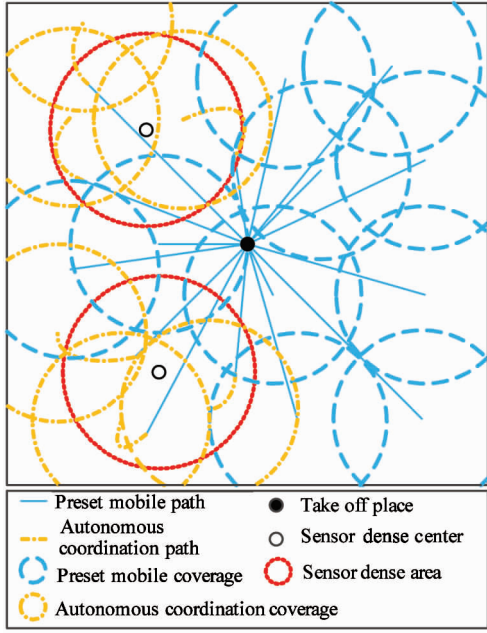


Fig. 3 Heterogeneous coverage results of MUAVSs

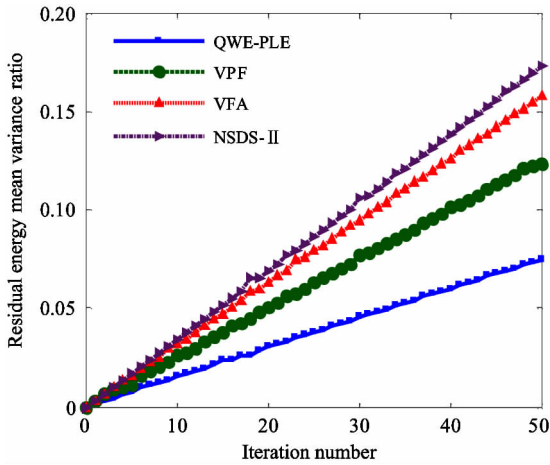


Fig. 4 Residual energy mean variance ratio transform with iteration

In Fig. 5, the algorithms show the changes of MUAVSs coverage with iterations. The QWE-PLE algorithm needs an overall plan about the 3 sub-objectives, so the coverage effect is lower than the others in the early stage. However, the effective coverage ratio is improved rapidly in the autonomous coordination stage, because the parameter PLE leads that the MUAVSs' mobiles refer to the sensor dense centers. Meanwhile, the non-sensor covered area is decreased. However, the compared methods tend to expand coverage

merely. While the energy holes appear, the original covering capability becomes weak rapidly. The experiment shows that the coverage ratio with the proposed method is 88.7%, which starts with the 36th iteration period. And the ratio is 10.2% higher than that with the compared methods at least.

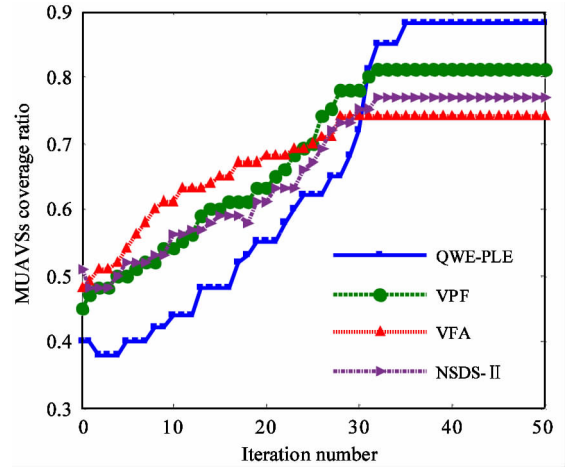


Fig. 5 MUAVSs coverage ratio transform with iteration

4 Conclusion

QWE-PLE algorithm with MUAVSs is presented based on quantum wolf pack evolution algorithm and power law entropy theory for heterogeneous sensors deployment environment. The proposed algorithm is composed of preset move and autonomous coordination stages, and satisfied 3 critical requirements. The experimental results show that the claimed method has great usefulness in non-repeated coverage, connectedness, and energy balance of sink layer.

References

- [1] Sharma V, Bennis M, Kumar R, UAV-assisted heterogeneous networks for capacity enhancement [J]. *IEEE Communications Letters*, 2016, 20(6): 1-4
- [2] Oubbati O S, Lakas A, Lagraa N, et al. CRUV: connectivity-based traffic density aware routing using UAVs for VANets [C]// *Proceedings of the 4th International Conference on Connected Vehicles & Expo*, Shenzhen, China, 2015: 19-23
- [3] Guo W, Devine C, Wang S. Performance analysis of micro unmanned airborne communication relays for cellular networks [C]// *2014 9th International Symposium on Communication Systems Networks & Digital Sign*, Manchester, UK, 2014: 658-663
- [4] Cesare K, Skeele R, Yoo S, et al. Multi-UAV exploration with limited communication and battery [C]// *Proceedings of the 2015 IEEE International Conference on Robotics and Automation (ICRA)*, Washington, USA, 2015: 1-6
- [5] Fan X G, Xu Z C, Che Z C, et al. A probabilistic barrier

- coverage model and effective construction scheme [J]. *Journal of Computer Research and Development*, 2017, 54 (5): 969-978
- [6] Ozdemir S, Attea B A, Khalil O A. Multi-objective clustered-based routing with coverage control in wireless sensor networks[J]. *Soft Computing*, 2013, 17(9): 1573-1584
- [7] Sabit H, Al-Anbuky A. Multivariate spatial condition mapping using subtractive fuzzy cluster means[J]. *Sensors*, 2014. 14(10): 18960-18981
- [8] Tiozzo G. Continuity of core entropy of quadratic polynomials[J]. *Inventiones Mathematicae*, 2014, 203 (3): 891-921
- [9] Ji P, Jiang J, Wu C, et al. A coverage detection and re-deployment algorithm in 3D directional sensor networks [C]//Proceedings of the 27th Chinese Control and Decision Conference (CCDC), Qingdao, China, 2015: 1137-1142
- [10] Ye G, Zhang B, Chai S, et al. Energy balanced redeployment algorithm for heterogeneous wireless sensor networks[J]. *Mathematical Problems in Engineering*, 2015, 6: 1-11
- [11] Khalesian M, Delavar M R. Wireless sensors deployment optimization using a constrained Pareto-based multi-objective evolutionary approach [J]. *Engineer Applications of Artificial Intelligence*, 2016, 53(6): 126-139
- [12] Xu D F, Pei X B, Bai Y, et al. Altitude information fusion method and experiment for UAV[J]. *High Technology Letters*, 2017, 23(2): 165-172
- [13] Qin D Y, Jia S, Yang S X, et al. Research on stateful public key based secure data aggregation model for wireless sensor networks[J]. *High Technology Letters*, 2017, 23(1): 38-47
- [14] Qiao G Y, Gao H B, Peng C, et al. Ground demonstration system based on in-orbit assembly oriented manipulator flexible force control [J]. *High Technology Letters*, 2017, 23(3): 271-278

Jin Shan, born in 1982. He is currently a Post-doctoral in School of Electrical and Information Engineering of Tianjin University. He received his Ph.D degree from Tianjin University in 2017. His research focuses on unmanned aerial vehicle, artificial intelligence, and coverage of wireless sensor networks.